Accepted Manuscript

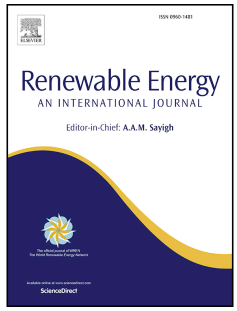

Numerical analysis for detecting head losses in trifurcations of high head in hydropower plants

Carlos Andrés Aguirre, Ramiro Gustavo Ramirez Camacho, Waldir de Oliveira, François Avellan

PII: S0960-1481(18)30818-8

DOI: 10.1016/j.renene.2018.07.021

Reference: RENE 10295

To appear in: *Renewable Energy*

Received Date: 26 June 2017

Revised Date: 1 June 2018

Accepted Date: 4 July 2018

Numerical Analysis for Detecting Head Losses in Trifurcations of High Head in Hydropower Plants

Carlos Andrés Aguirre[1], aguirrerodriguezandres@gmail.com
Ramiro Gustavo Ramirez Camacho[1,2], ramirez@unifei.edu.br
Waldir de Oliveira[1], waldir@unifei.edu.br
François Avellan[2], francois.avellan@epfl.ch

1 Itajubá University Federal, Institute of Mechanical Engineering. MG, Brazil, CEP 37500-901
AV. BPS, 1303, Bairro Pinheirinho, Itajubá – MG, Telefone: (35) 3629 - 1101 Fax: (35) 3622 – 3596
2 EPFL, École Polytechnique Fédérale de Lausanne, Laboratory for Hydraulic Machines, Switzerland.

Abstract. *Many different types of branching have been developed, such as bifurcation, trifurcation, and manifolds, among others. These configurations are used in penstocks to transport water from surge tanks to power houses in order to feed several turbines at the same time. This arrangement allows for smaller assembly costs in comparison with independent penstock systems. Nevertheless, such installations can generate higher head losses in the system in comparison with single systems. This study focuses on the quantification of these head losses as a function of volumetric flow rate using Computational Fluid Dynamics (CFD) and later validated with previously published results. To determine the coefficient of head losses three mesh settings were analyzed: hexahedral, tetrahedral and hybrid, for both a steady state and transitory flow. Based on the literature, the k-ω turbulence model was used, with refinement to elements near the wall to check y+. To the simulation transitory, the SAS model was used for analysis of the instability in the trifurcation.*

Keyword: Trifurcation, CFD, Loss coefficient, SAS, Transient

1. Introduction

Extensive research has been carried out in order to quantify losses in adduction systems, particularly in the high pressure components of hydroelectric plants in order to maximize their performance. Common types of branching seen in studies are bifurcations, while a few studies have looked into trifurcations in penstocks. This can be attributed to the uneven flow at the turbine entrances and higher variable loss coefficients. It is important to note that turbine performance depends on the flow behavior on the penstock, and therefore the research on trifurcations could be made through numerical or experimental analyses to provide vital information for an appropriate turbine design. In hydroelectric plants that only use one penstock, it is essential to use branches for the flow distribution of the hydraulic machines. Three geometric configurations of the ramifications are mainly used in penstocks; bifurcations, trifurcations and manifolds. The bifurcations and trifurcations can be classified into two categories based on the geometry employed, considering the structural advantages. The first geometrical arrangement is comprised by trunk cones which intersect in the middle of the branches, while the second geometry uses a sphere between at the branches.

Both geometrical arrangements need to be designed carefully to enable an even flow, avoiding excessive pressure drops, vibration and cavitation [1]. Other important design aspects to take into account for the pressure loss are the geometrical supports that reinforces the branches, the branching angles, the transition between the penstock and the branches (expansion and contraction). It is important to highlight the relationships between these design aspects and the construction limitations.

An early research study focused on the analysis of load losses caused by the geometric variations of branches in a pipe, and was carried out by Petermann cited in Mayr [2]. Gladwell and Tinney [3], conducted a study of the trifurcation of Round Butte project of 367 MW in the United States. Cone trunk geometry was analyzed through several tests applying changes to the input conditions by changing the flow and output for each branch, the branch being kept open or closed. This study enabled the detection of vortex formations due to the separation of the boundary layer in the clearance section of the lateral branches, so it was possible to obtain the pressure drop curves in the various settings. The results of the coefficients in the xxx configuration were in the range from 0.45 to 0.55 for the side branches, and from 0.37 to 0.47 in the central branch. The symbol xxx, was based on the reference from Gladwell and Tinney [3], representing the situation with three open branches and xox represent the lateral branches opened and the central closed (x = opened, o = closed)

Berner [4], realized tests in a trifurcation geometrical model with cone trunks and a taper angle of 24°. The loss coefficients obtained for the configuration of the three open outputs were as follows: 0.123 in the left branch; -0.12 the central branch; and 0.104 in the right branch. In the second part a comparison was made between the trifurcation and an arrangement of two forks in order to supply three hydraulic machines. The results showed that the use of trifurcation is more favorable for the smaller load loss coefficients.

At this point it is important to conduct analysis related to the negative coefficients in trifurcations and bifurcations, defined by an anomaly, because there should not be any negative energy loss due to the principle of energy conservation. Investigators have suggested that this may be due to the non-inclusion of kinetic energy coefficient in the computations of energy losses without any experimental evidence. In the technical note by Rao and Kumar [5], experimental analysis was performed to evaluate the velocity profiles and the energy loss coefficients, by correcting the kinetic energy coefficient based on the integration of the velocity profiles, concluding that there is no loss of negative energy in the central branch. As highlighted by Wood et al [6] and Liggett [7], use of the term 'loss coefficient' is therefore somewhat inaccurate, since its value is affected by energy exchange as well as energy loss. However, following Wood et al [6], the term is retained, given its widespread use.

The trifurcation of Marsyangdi Hydroelectric 70 MW in Nepal was tested by Richter [8], with a model in 1:20 scale, the trifurcation having a spherical geometry. The loss coefficients in the central branch to the configuration of the three open outputs were 0.11. The pressure loss coefficients of the lateral branches were identical, recording a value of 0.61. The energy losses were higher in the side branches, due to the formation of vortices in the flow ball and the reverse flow region. If the ball size is greater, instabilities of the vortices will be greater. Other experimental analyses and numerical simulations with various changes in geometry and some simplifications on the permanent and non-permanent arrangements have been made.

Tate and Mcgee [9] made a model in 1:25 scale with geometry cone trunks for the experimental analysis of the Hydroelectric trifurcation of Fort Peck Dam 185 MW in the United States. The central branch of the loss coefficients operating in "xxx" configuration with various flow rates have negative values of -0.10. For lateral branches the load loss coefficient is in the range of 0.24 to 0.63 depending on the changing flow rate.

Mayr [2] conducted the analysis of a hydroelectric plant in Musi where the conditions in the input trifurcation were the flow rate of approximately 0.3 m³/s, atmospheric pressure, the flow at the entrance can be fully axial or induced spin, configuration "xxx" test (the three branches open). The pressure loss coefficient of lateral branches changed between 0.32 and 0.4 and for the central branch between -0.177 and -0.178.

Some analyses have also studied the function of the flow rate output variation of pressure loss coefficient or non-permanent regimen versus time as Ruprecht et al., [10] in the trifurcation of the Marsyangdi Hydroelectric and Tate and Mcgee [9] in the Power of Fort Peck Dam.

2. Trifurcation

For this analysis the flow field and geometry of Gurara-Nigeria trifurcation were used in accordance with the operating conditions of pressure, flow mass and thermodynamic properties such as bulk density and dynamic viscosity of the flow. A mesh study is made using three meshes with different amounts and types of elements. Based on convergence criteria, computational cost and quality elements, these variables defined the mesh type based on the solution criteria that depend on the number of elements. After this analysis, the loss factors are analyzed for different flows and trifurcation geometries. Finally, through post-processing the local and global results are obtained as a pressure variation in transient model.

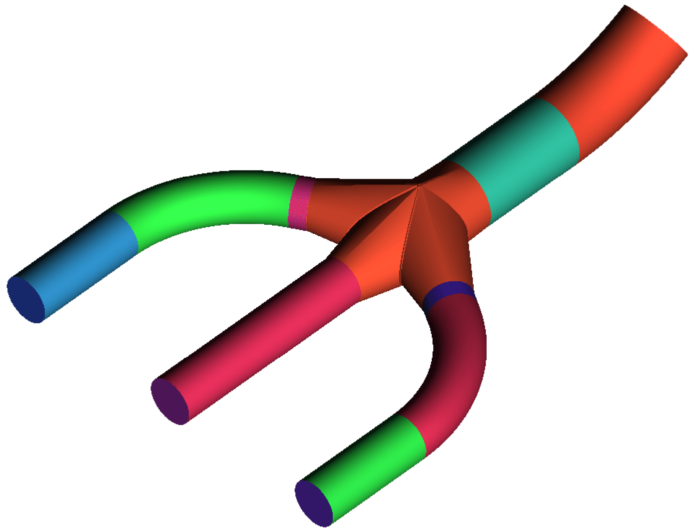

Figure 1 - Geometry of Trifurcation (Gurara Nigeria).

2.1 Geometry and boundary conditions

Trifurcation geometry used in this study was provided by ALSTOM®. This company was part of the first construction phase of the hydroelectric plant in Gurara, Nigeria (30 MW). The geometry is initially composed of a loading chamber, a high pressure tube and the trifurcation. Only trifurcation is analyzed due to the large number of elements that would be required to discretize the loading chamber and pipe volumes. The volume is therefore only defined for the trifurcation by its two elbows on the lateral branches and an elbow on the inlet pipe (Figure 1), commonly used in trifurcation projects.

The diameter of the pipe at the entrance is 4.5 m, while in the ramifications, it is 3 m. The Gurara trifurcation is comprised by the trunks of the cone, and its particular geometrical features are shown in Figure 2. The geometrical dimensions of the trifurcation can be determined by the opening angle of 60°. This value is appropriate especially in the middle of the range of allowed values of 45° up to 75°. The taper angles are varied according to their location (cone length), and most of them are outside the range of recommended values, that is, 6° to 8°. The taper angles are related to the lengths of the cones through the ratio of diameters, which for trifurcation Gurara is 1.5, this relation being the highest when compared to other designs where the area ratio is around 1.0 (area of the principal tube and area of the ramifications). The other geometric aspect that affects the yield is the mechanical supports of the trifurcation, which penetrates the internal control volume of 0.5 m with a thickness of 0.12 m, as can be seen in Figure 2.

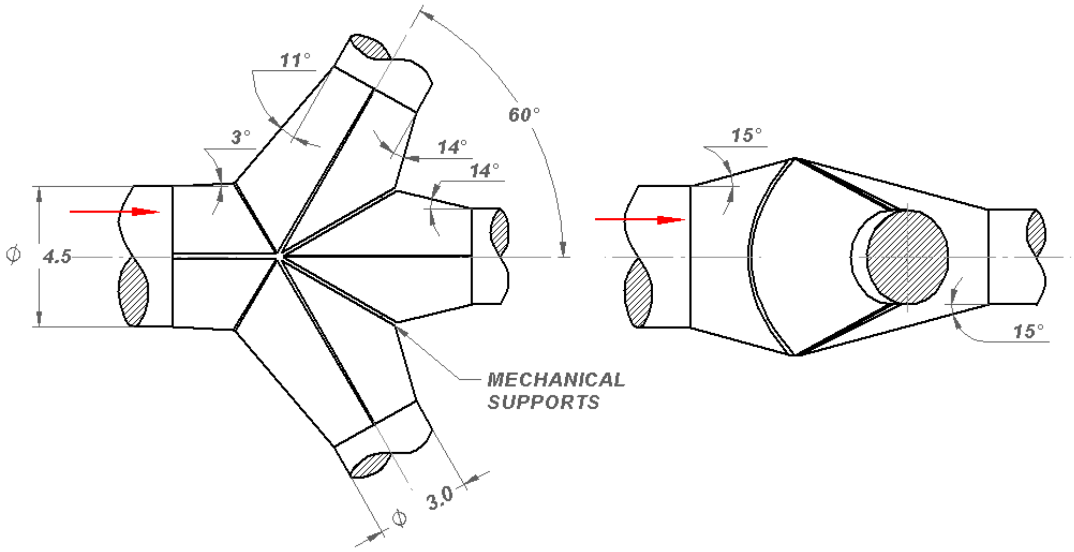

Figure 2. Dimension of trifurcation Gurara – Nigeria.

The fluid inside the trifurcation is water at 25 °C and with a specific mass of 997 kg/m³. In the design point, the volumetric flow is 90 m³/s, and the pressure of the reservoir water column is not taken into account, since the total pressure difference and the pressure drop will not be affected. Therefore, the boundary conditions state that: in the entrance is the mass flow rate and the average static pressure in the ramifications outlet, and friction losses are considered, assuming a hydraulically smooth wall.

3 Mesh analysis

The numerical analysis of trifurcation depends on the generation and development of a mesh that allows the discretization of the control volume and also attains an accurate description of the turbulence phenomena. It is essential that the mesh has a high quality, considering the flow transitory. The three initial mesh alternatives are hexahedral (structured), tetrahedral (unstructured) and hybrid with hexahedral core. The two main conditions imposed on the mesh are the quality and y+ to set the element size near the wall.

The recommended values for the y + require the turbulence model to be used in the numerical analysis and the model applied in the wall functions for the flow in the boundary layer. For Joeppen [11] and Casartelli et al. [12], trifurcations and penstocks, respectively, the k-ω SST model is the most suitable option for flows with reverse flow in continuous and complex geometries.

The size of the first element has to be within the log-law region. For the k-ω SST model the range is between 60 < y+ < 300 depending on the Reynolds number and use of wall functions. This model allows for automatic variation~~,~~ between scalable wall functions and other functions for regions of low and high Reynolds numbers [12]. Therefore, the chosen y+ is around 300, considering the flow characteristics, in order to obtain the meshes with moderate numbers of elements, while taking advantage of the wall functions for an appropriate solution of the boundary layer.

Using the ICEM-CFD® it is possible to generate the three types of meshes, for which the number of elements is shown in Table 1.

Table 1 - Mesh types and number of elements

Mesh Type	Number of elements	Geometrical quality*
Hexaedrical	6.911.165	99.980 % > 0.3
Tetraedrical	7.067.766	99.311 % > 0.3
Hybrid	5.749.921	98.821 % > 0.3

* Optimum quality =1.0 according [12].

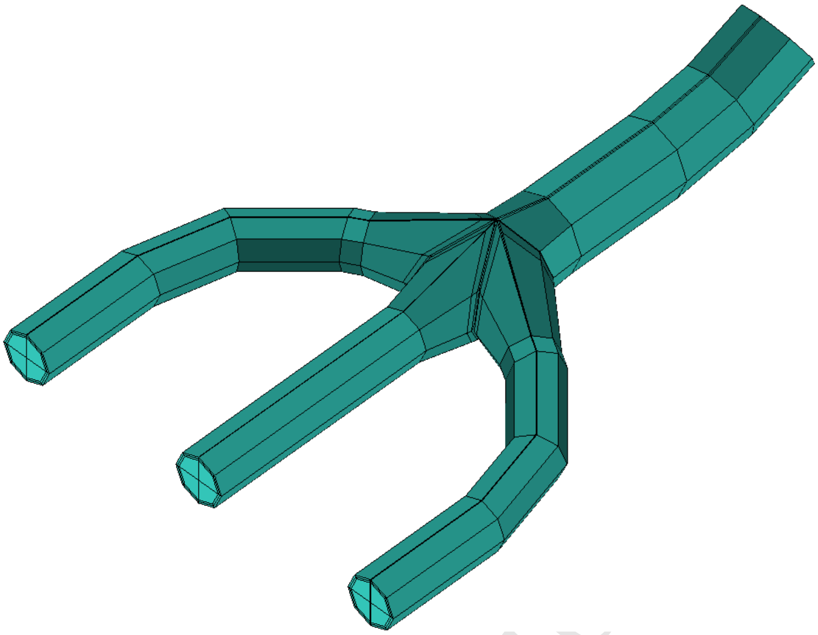

Figure 3a.- Block configuration for hexahedral mesh generation

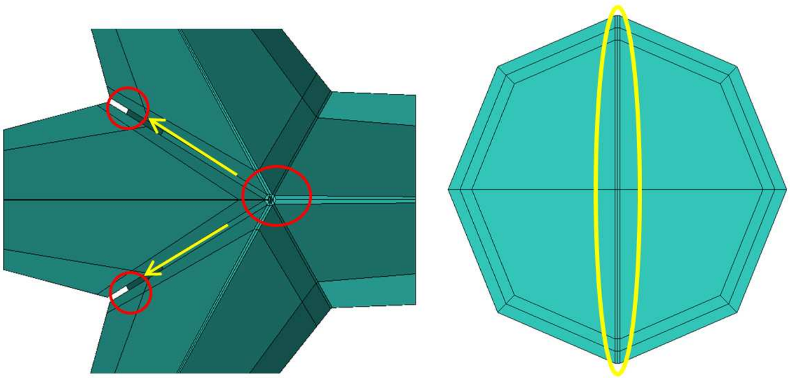

Figure 3b.- High and low density element regions

The hexahedral mesh was constructed with 844 blocks and 28 layers with linear growth in the outer wall of the trifurcation "O-grid", taking into account the value of y+, seen in Figure 3a-b. The overall quality of the mesh elements is higher than 0.3, which is the minimum recommended for all meshes in ICEM-CFD®.

The preparation of the hexahedral mesh was a great challenge due to the geometry at the junction of the four pipes. In this region, it was necessary to use a large number of small blocks and double "O-grids". In Figure 3, the red lines represent regions that are critical for refinement of the mesh, and the yellow lines the regions where high refinements are not necessary, and therefore a controlled transition from the size of elements between these regions was performed in order to minimize numerical errors.

The second mesh (unstructured) is composed of tetrahedrons and pyramids, with fifteen prismatic layers near the wall of linear increase of 1.3. The third mesh (hybrid) is composed of hexahedral and pyramids in the core and 18 prism layers near the wall. Figure 4(a) shows the effect of hexahedral mesh refinement at the walls of the mechanical supports and how the propagation of high densities of elements within the mesh is attenuated using linear growth of the elements. In unstructured (4b) and hybrid (4c) meshes, refinement layers were used to raise the density of elements near the wall without propagation inside the dome. The three generated meshes are evaluated considering a steady flow for the range between 20 m^3/s up to 65 m^3/s, using the solver ANSYS - CFX®. The convergence value is the RMS (root mean square) set at $1x10^{-4}$.

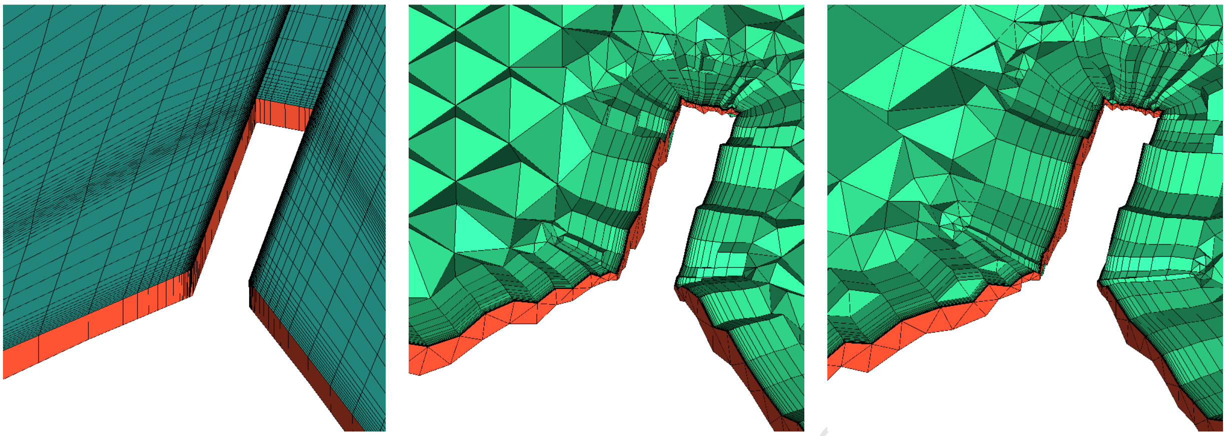

Figure 4- Refinement a) Hexahedral mesh, b) Tetrahedral and prismatic mesh c) Hybrid mesh

3.1 Loss Coefficient Analysis

Using the three configurations, a loss coefficient analysis was conducted for the mass flow rate varying between 10 m^3/s to 60 m^3/s. Figure 5 shows the differences in the value of loss coefficient in the lateral ramification, comparing the hexahedral mesh with the tetrahedral mesh. In the central ramification there are no great differences in the loss coefficient.

The loss coefficient was defined by the expression;

$$\zeta = \frac{\Delta P_T}{U^2 / 2g} \qquad (1)$$

Where ΔP_T, is the difference of total pressure; U is the reference velocity that, according to Ahmed [1], Dobler [13], Lasminto [14], Wang [15] and others, the value of velocity U is applied in the inlet tube of the trifurcation.

It is important that the convergence by hexahedral mesh reached $10x10^{-5}$ RMS. Figure 5 shows the behavior of the loss coefficient as a function of the volumetric flow. The computational costs for the three meshes are similar, because although the hexahedral mesh reaches convergence with a smaller number of iterations, the time iteration remains the largest compared to the other types of meshes. The time used for the tetrahedral and hybrid meshes per iteration is lower, but requires more iterations to reach convergence. The computational time has been verified as shown in Table 2. Here a cluster of 36 cores was used, IntelXeon®64, 2.6 GHz and 128 GB Ram in the Virtual Hydraulic Laboratory LHV– Mechanical Institute (UNIFEI).

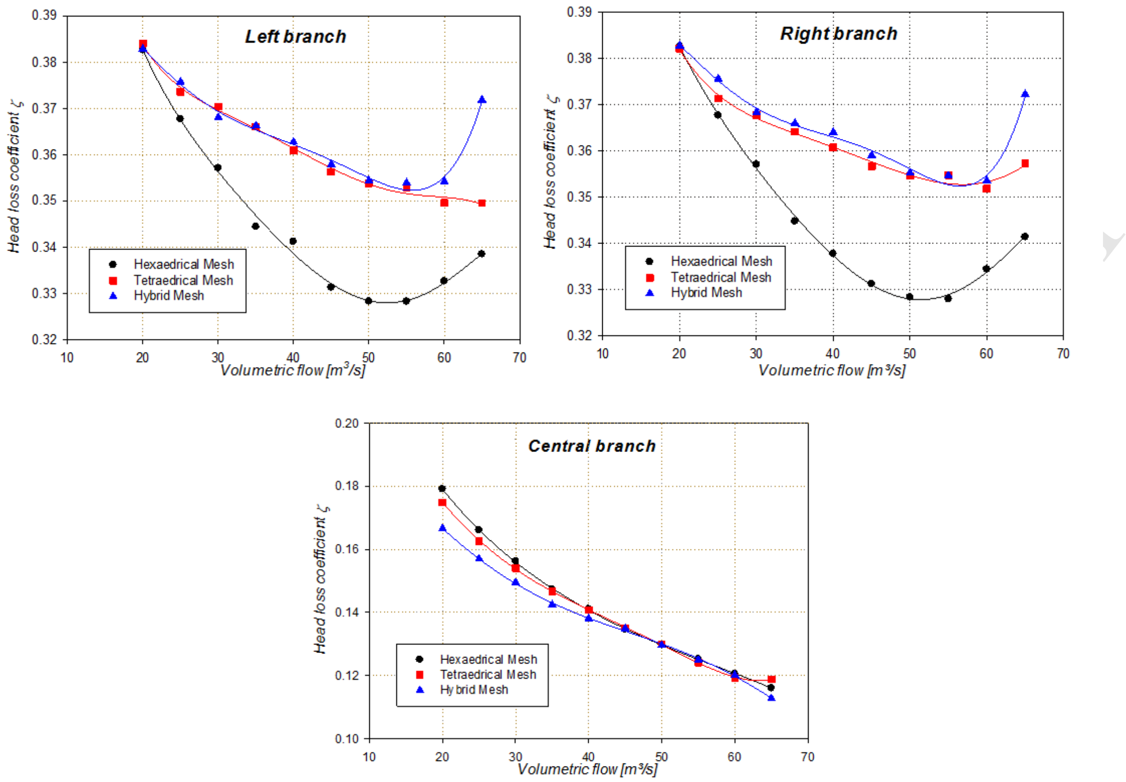

Figure 5.- Loss coefficient for three mesh configurations

Table 2- Computational cost for three mesh configurations

Flow [m^3/s]	Hexaedrical mesh		Tetraedrical mesh		Hybrid mesh	
	Iterations*	Time [s]**	Iterations*	Time [s]**	Iterations*	Time [s]**
20	80	35.155	150	18.280	200	16.618
40	80	34.172	170	17.401	160	17.408
60	100	36.532	190	17.786	180	16.580

*Number of iterations to attain a convergence of 10-4 ** Time used in one iteration

When the three analyses were made, the mesh that provides the best accuracy in the results with a reasonable computational cost can be chosen. According to these mesh parameters, the hexametrical mesh provides the most appropriate conditions to continue with the study of trifurcation. However, the results obtained using the hexahedral mesh depend on the numerical errors generated by the mesh. In order to minimize the dependence of the results on the refinement of the mesh, an independent analysis is carried out.

The initial mesh hexahedral "M", the number of elements is changed, mainly near the wall. According to Cox-Stouffer [16] in the modified first mesh "M_{low}" the number of elements must be reduced and for the second "M_{high}" a further refinement of the mesh should be made and quantified using the loss coefficient. The results for selecting the mesh are shown in Table 3.

Table 3 - Analysis for selecting the mesh by loss coefficient.

Mesh	Volume	y+ (*)	Loss coefficient ζ			Relative error %		
			Left	Central	Right	Left	Central	Right
M_{low}	5.550.987	≅402.75	0.3483	0.1033	0.3444	-	-	-
M	6.911.165	≅277.08	0.3471	0.1014	0.3484	0.3457	1.8737	1.1481
M_{high}	8.932.761	≅219.75	0.3461	0.1008	0.3499	0.2881	0.5952	0.4305

* mean value of y calculated in different surfaces

Table 3 shows the percentage relative error values, in reference to mesh M. The convergence criterion requires a variation of less than 1% for the loss coefficient, which means that the value between the data obtained from a coarser mesh and a more refined mesh is less than 1% of the initial value of loss coefficient. This criterion is widely used in academic research, such as Fonseca et al. [17], and Vinchurkar Longest [18], among others. Considering the data in Table 3, the "M"-mesh gives loss coefficients load which do not change significantly with a further refinement, thus indicating that the mesh meets the independence criteria. Thus the M-mesh was used.

The examination of the spatial convergence of a simulation for determining the discretization error on CFD simulation is also important. Roache's [19] report shows the criteria of GCI (Grid Convergence Index). For testing this criterion, the program can be used to verify.f90 [20] for three types of mesh based on the results in Table 3 (for example the left branch). Results show the value of the asymptotic range equal to 1.034652, a value near 1.0. Likewise the Richardson extrapolation result is 0.3411010, and the grid convergence Index (GCI) Refinement ratio M_{low}:M=2.583638% and Refinement ratio M:M_{high}=2.080862 values are considered low, and as such, it can be concluded that the use of mesh M was more appropriate taking into account the high computational cost.

The first approach to quantify the pressure loss coefficient is based on the optimal flow conditions, axial inlet with velocities of a uniform profile. These results attend to comparisons and evaluations with other settings by trifurcations.

The range of flow rates examined extends from 20 m^3/s up to 105 m^3/s, while the data obtained at around 105 m^3/s can still be considered as steady. However, it was observed in the calculation of convergence of the solution what appears to indicate the transitory phenomena, which is to be analyzed further in this study. The results are presented in Figure 6, with flow increments of 2.5 m^3/s for a total of 35 flows employed in the creation curve.

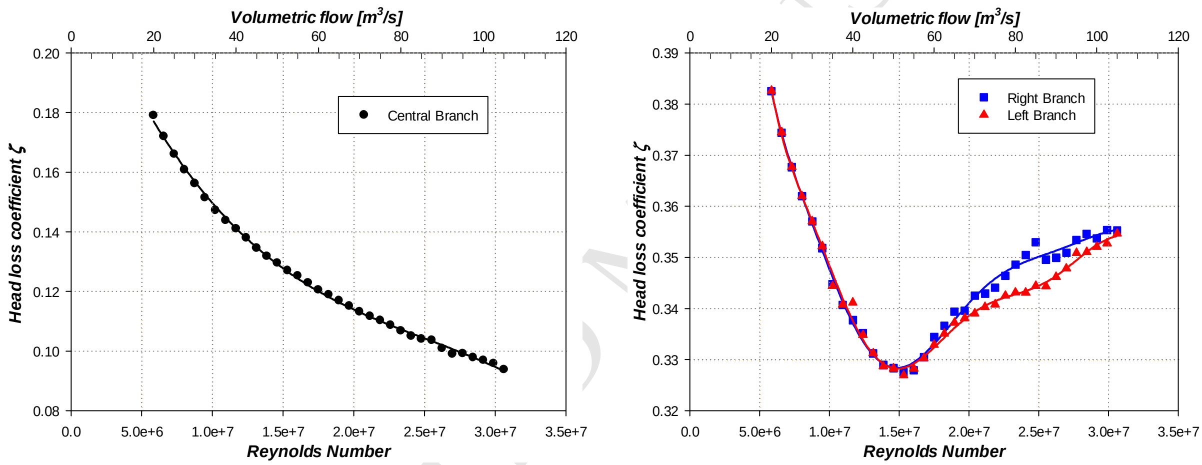

Figure 6 - Loss coefficient vs. volumetric flow and Reynolds number for the central and side ramification

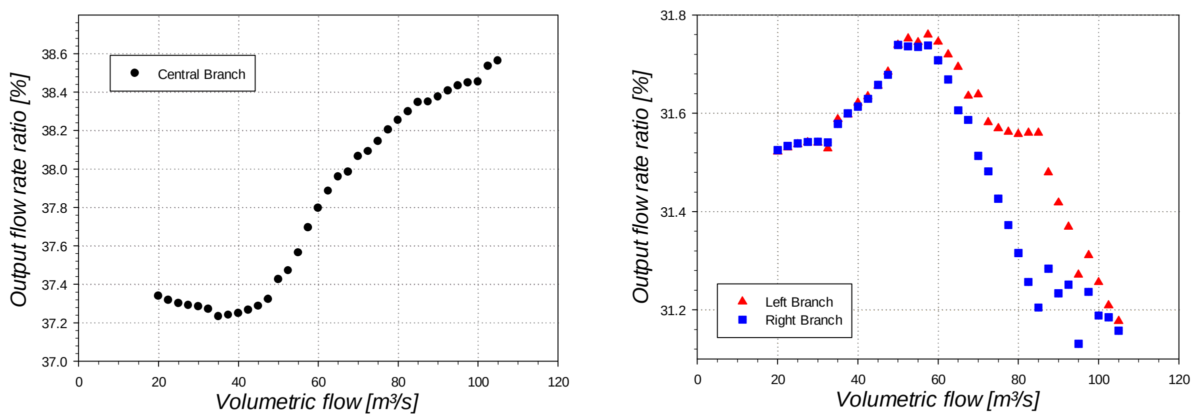

Figure 7 - Variation of the volumetric flow in the trifurcation, a) central b) left and right branches

Figure 7 shows the flow volumetric distribution in percentages for each ramification. To have an equal distribution, this value must be around 33.33%, which, however, is impossible. Therefore, the regulation system of the turbine should control the flow considering three equal machines.

The superior cupule is the region where the high variations in the flow originate are formed. It can be seen in Figure 7 that for the central and lateral ramifications for high values of flow (around 60 m^3/s) minor variations of 37% are observed in the central ramification, and around 31%, for the left and right ramifications. In such a situation, the regulation system should operate to retain the volumetric flow equally distributed, since no high instabilities exist in the transitory flow.

The development of trifurcation follows particular characteristics of each design, resulting in different geometries, even when all of them perform the same function. When the values of the ratio of diameters, pressure or flow are changed, the coefficients and the percentage of flow can have clear variations in the results. Therefore, a strict validation of the results obtained numerically for the trifurcation of Gurara Nigeria - ALSTOM® can only be made by verifying the scale model with experimental data. However, it is possible to make a qualitative validation based on other similar trifurcations. In order to generalize the results to the particular conditions of each trifurcation, the loss coefficient is related to the Reynolds number of the permanent system, and for the non-steady state is made according to the variation in total time and the loss coefficient.

In literature, for trifurcations in steady state, only values for pressure loss coefficients are presented, so other comparisons are improbable. Studies or analyses that provide the data desired to make the comparison are presented in Table 4, including the results of this study to the design point of 90 m³/s.

Table 4 – Experimental results of the loss coefficient in different trifurcations settings

Design	Author	Year	Geometry	D_i/D_o	α	Re*	Coefficient ζ		
							R_{left}	$R_{central}$	R_{Right}
Round Butte	Gladwell	1965	Conical	1.75	45°	$2.50x10^7$	0.450	0.380	0.540
N-D	Berner	1970	Conical	1.82	50°	$3.00x10^6$	0.123	-0.120	0.104
Marsyangdi	Richter	1988	Spherical	1.78	75°	$2.53x10^7$	0.610	0.110	0.610
Musi	Klasinc	1998	Spherical	1.66	60°	$2.24x10^7$	0.295 – 0.311	-0.120 – -0.118	0.295 – 0.311
Marsyangdi	Mayr	2002	Spherical	1.78	75°	$2.53x10^7$	0.232 – 0.274	-0.023 – 0.016	0.232 – 0.274
Musi	Mayr	2002	Spherical	1.66	60°	$1.63x10^7$	0.342 – 0.414	-0.178 – -0.177	0.382 – 0.386
Gurara	Aguirre**	2015	Conical	1.50	60°	$2.54x10^7$	0.346	0.100	0.349

* Number Reynold in the design point ** Numerical result

Figure 8 shows the graphs of the pressure loss coefficients for the central branch and Figure 9 for the lateral branches (based on Table 4). The loss coefficients of the central, left and right branches are represented by black, red and blue colors respectively. The green color in Figure 9 indicates when those coefficients are equal for the two lateral branches. The error bars indicate the range values.

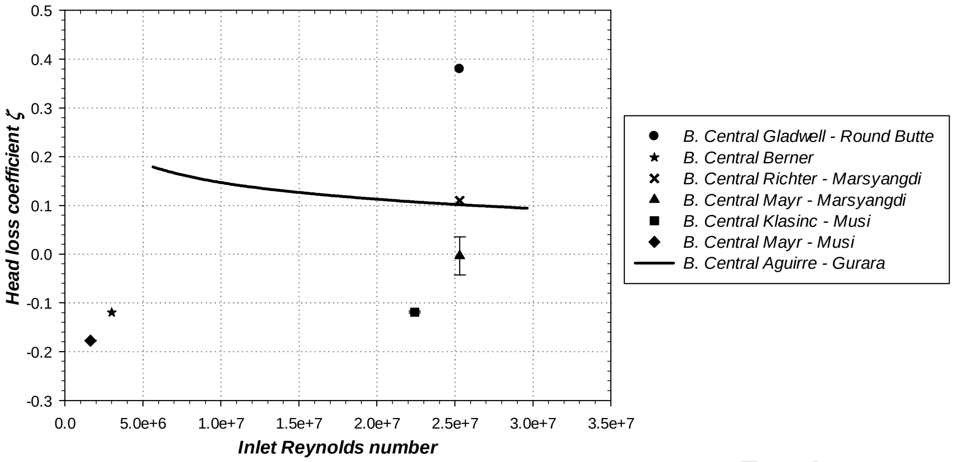

Figure 8 - Pressure loss coefficients in the central branch, according to various authors and geometries

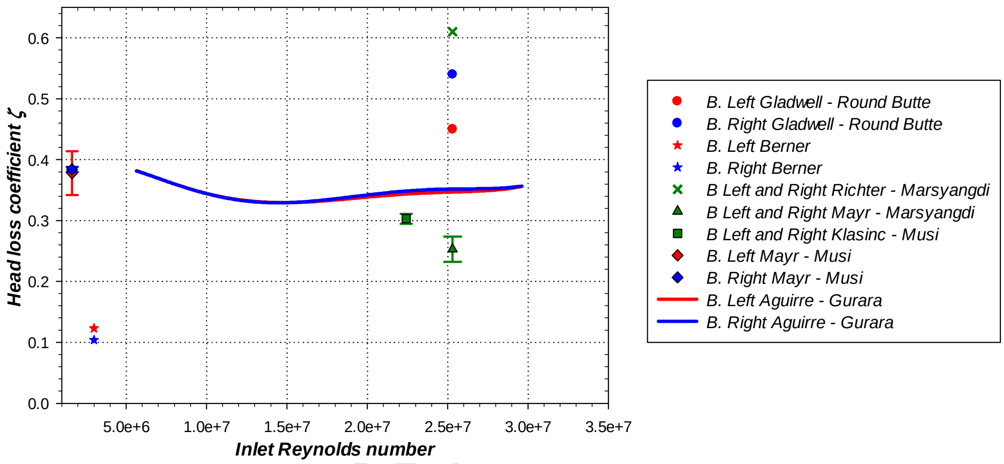

Figure 9- Pressure loss coefficients in the lateral branches, according to various authors and geometries

All coefficients for the central trifurcation are in a range between -0.2 and 0.4. Some of these coefficients are negative, which is not a realistic situation but which is often observed in experimental tests, such as in this case, when there is an increase in the rate at the central branch.

The Musi project study made by Klasinc et al. [21] is more related to the operating conditions and geometry of the trifurcation Gurara-Nigeria. Comparing the results of the coefficients to the central branch, these are very close, with a variation of only 0.2. The coefficients obtained for the side branches have a higher compliance; there is a difference of approximately 0.05 for the Reynolds number used by Klasinc et al. [21]. The difference between the trifurcation results of the Gurara-study is mainly justified by the geometry, where there are similarities; nonetheless, they are not identical.

In the trifurcations analyzed by Gladwell et al. [3] and Richter [5] the loss coefficients were higher for the three branches having different geometries but with the diameters ratios being similar. The smaller coefficients for the three branches were obtained by Berner [4], with a diameter ratio similar to that trifurcations with the higher loss coefficient.

3.2 Unsteady Analysis of the Pressure Loss Coefficient

The analysis of the pressure loss coefficient for the trifurcation, in non-steady state is defined with following parameters recommended for SAS SST turbulence model; the time-step is defined from the criterion of Courant-Friedrichs-Lewy (CFL) given by Equation 2, the recommended values for the CFL number being in the range between 0.5 and 1 or even lower according to the computational resources (ANSYS INC., 2012). The comparison of the LES and SAS-SST models, made by Menter and Egorov [22], highlighted that the SAS-SST model is more efficient to solve the turbulent flows using CFL ~ 1 as a criterion. Even with less refined meshes these results are similar to URANS approaches, while the LES and DES models in this condition provide less than satisfactory results.

$$CFL = \frac{U\Delta t}{\Delta x} \tag{2}$$

The velocity U is given in the axial direction of the trifurcation considering the volumetric flow on the design point; Δx is determined by the average value of the length of the mesh elements in the normal direction in the inlet and Δt is the time step value, for which the initial value was 0.020 s, but to ensure the recommended CFL-criterion this was reduced to 0.010 s. With this time-step calculated, CFL = 0.48, which is lower than the range of minimum requirements.

The maximum number of iterations is restricted by the computational cost. Given these restrictions, the total time employed was 50 s. The first 20 seconds are not considered, because these do not yet correspond to the transitory state. The boundary conditions are similar to those used in steady state. The point analyzed is 90 m^3/s (design point). The numerical schemes are chosen according to the ANSYS-CFX® recommendations, the SAS-SST model uses Central Difference scheme in the regions where it employs the LES model and in the stable regions where it operates as RANS or URANS, the High Resolution model applies, which can be set by the user.

This function that mixes the two schemes of permanent and non-permanent arrangements are known as Central Difference Scheme Blending. The scheme for the transitional term is determined by the user in this case, and the High Resolution Transient scheme is applied, which provides the ability to quickly switch between the Backward Euler schemes of first and second degree, when possible. The convergence criterion is $1.0\text{x}10^{-5}$, to all variables. Calculations of the pressure loss coefficient and the flows are made as shown in the steady state. Head loss coefficients obtained in non-steady state are shown in Figure 10.

3.3 Analysis of Vortex Flow

The effects of the vortices in the pressure loss coefficient can be evaluated with an analysis on their formation, propagation and dissipation in the flow. The connection between the vortices and the loss coefficient depends on the development of turbulent flow at the time, since this induces the formation of such structures. The schemes to identify and visualize these structures are different, and each author has a different method to accurately recognize a wider range of vorticity flows.

The vortices are considered coherent structures; a more particular definition for eddies and causing the rotary motion of a mass or quantity of particulate matter around a central point. This definition describes the vortices in coils that are represented by current lines or iso-contours of vorticity around regions of pressure minimum and constant pressure, but these representations may have similar movements, even when they do not exist [23],[24].

Analyses of vorticity have different approaches employed for describing the velocity field as: Q, λ2 and Δ, to identify vortices in two and three dimensions (ANSYS INC., 2012). Initially the analyses in two dimensions and in the steady state can be made using the vectors of velocity in longitudinal planes, where one can identify the vortices as the flow vectors rotating around a point (ANSYS INC., 2012 reference manual). The problem with this method is that it provides little information to identify vortices in three dimensions.

The criterion Q uses the velocity gradient tensor D, which is decomposed into two parts: symmetrical and non-symmetrical, given by deformation S and vorticity tensor Ω respectively. This decomposition is presented in Equation 3.

$$D_{ij} = S_{ij} + \Omega_{ij} \qquad where, \qquad S_{ij} = \frac{1}{2}\left(\frac{\partial U_i}{\partial x_j} + \frac{\partial U_j}{\partial x_i}\right) \quad e \quad \Omega_{ij} = \frac{1}{2}\left(\frac{\partial U_i}{\partial x_j} - \frac{\partial U_j}{\partial x_i}\right) \tag{3}$$

The criterion Q represents the local balance of the strain rate and magnitude of vorticity, defining vortices as regions where the magnitude of the vorticity is greater than the magnitude of deformation [24]. This can be expressed as in Equation 4.

$$Q_{Dim} = C_Q\left(\Omega^2 - S^2\right) \qquad where, \qquad S = \sqrt{2S_{ij}S_{ij}} \quad e \quad \Omega = \sqrt{2\omega_{ij}\omega_{ij}} \tag{4}$$

The values of Q change according to the software used, which for ANSYS, FLUENT® is 0.5 and for ANSYS-CFX® is 0.25. This criterion provides good results, for the identification of the vortex when used in incompressible flow. The Q values are very different for high Reynolds numbers reaching $1\text{x}10^8$. In the analyses of

Q, for iso-surfaces it is not necessary to use values negative or equal to zero, since they only represent weak structures or unimportant for the analysis of turbulence (ANSYS INC, 2012d).

The values of the head loss coefficients vary between 0.003 and 0.131 for central branching and between 0.331 and 0.538 for the side branching. The average value of the coefficient in the time interval shown in Figure 10 is 0.067 in the central branch and 0.459 and 0.454 on the left and right respectively.

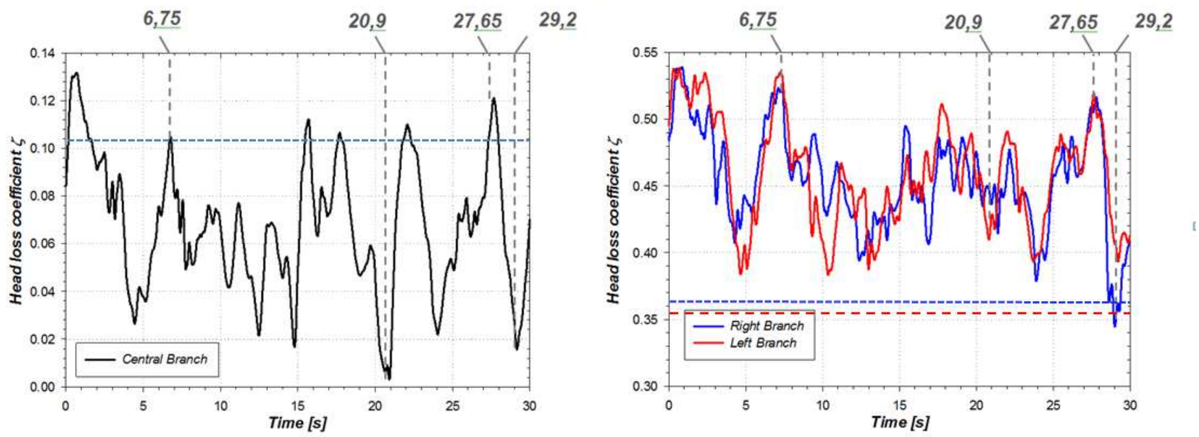

Figure 10 - Temporal variations in loss coefficient in the central and lateral ramifications, volumetric flow 90 m³/s, the dash line representing the solution in steady state

Comparing the values and the intervals of the head loss coefficients in permanent and non-permanent schemes, it is possible that the coefficient of the central branch in steady time 0.100 is within the non-permanent range (0.003 and 0.131). For the lateral branches, i.e., left and right branches, the coefficients are 0.346 and 0.349 in steady time, which are very close to the lower limit of the non-permanent scheme, around 0.45, and therefore the average coefficients in transient, show that the loss coefficient is slightly larger when compared with the result in steady time.

The analysis of vortices in three dimensions can then be shown using Q iso-surfaces in the limits of the pressure loss coefficient ranges, with reference to Figure 10, and this is shown in Figures 11 and 12.

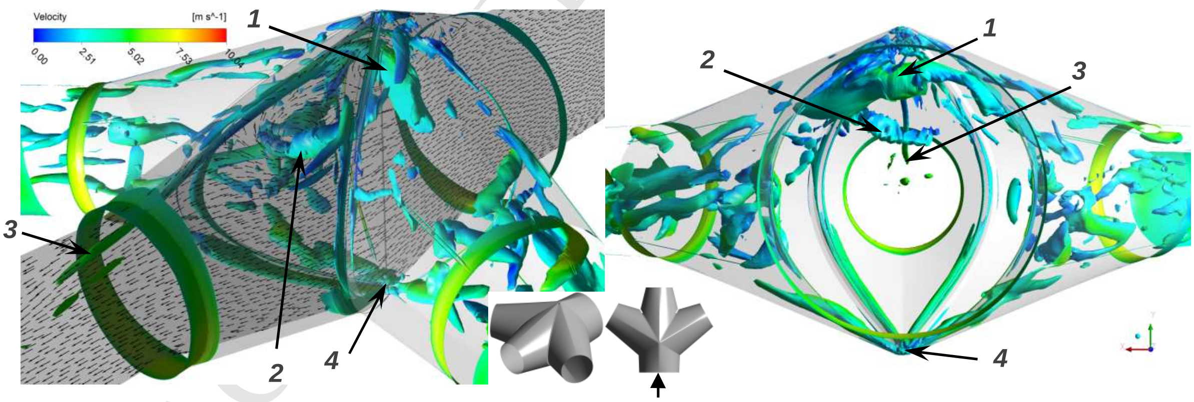

Figure 11 - Turbulence structures for the time 6.75 s. Iso-surface Q = 50 s^{-2} and velocity contour (see the color maps)

Figure 11 shows the formation of vortex 1 at the top of the trifurcation between the lateral branches. The intensity given by the velocity contours is high in vortex 1 compared with the closest one to vortex 2. Vortex 3 is stretched by the flow and has a velocity variation between the dome and the trifurcation central branch. At the point below 4, originating from the trifurcation, four structures arise: two in the direction of the lateral branches and the remaining two circulating in the interior supports of the trifurcation.

Another time instant with similar characteristics to the time of 6.75, which is 27.65 s, has high values of head loss coefficient for the three branches, the distribution of the vortices being shown in Figure 12. One difference is the formation of a second, smaller vortex near vortex 1 at the top of the trifurcation. In this figure one can observe the lateral vortices, particularly in the right branch, and vortex 3 is already greatly reduced.

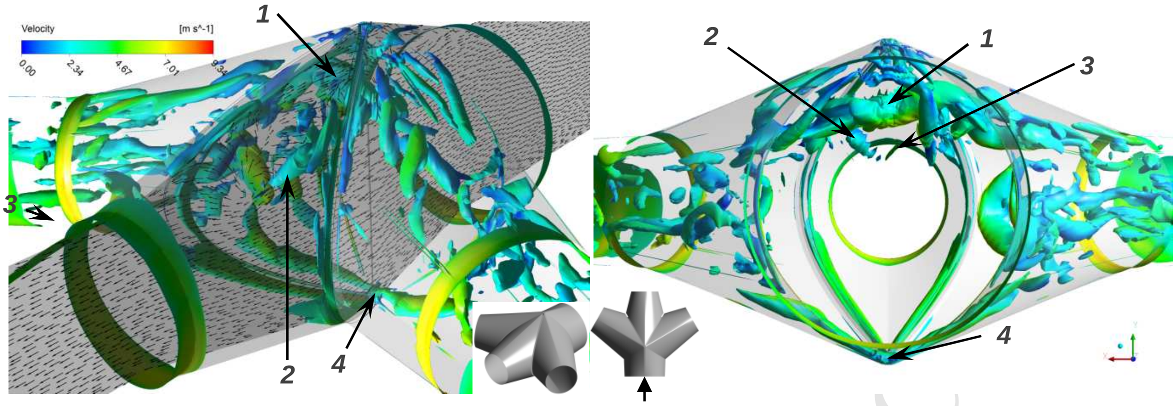

Figure 12 - Turbulence structures for the time 27,65 s. Iso-surface Q = 50 s-² and velocity contour (see the color maps)

At the time instant of 20.9 s, the coefficients were reduced mainly to the central branch, reaching a value close to zero. The smaller vortices that induce this behavior are shown in Figure 13.

This analysis can be better observed when the time evolution is accomplished through a video, where all vortices related to the loss coefficient can be identified. The turbulence SAS model is appropriate in this situation considering the y+ parameter, and the mesh construction criteria, as seen in item 3.2.

The outlet volumetric flow in each ramification presents fluctuations tightly rationed as obstruction by large vortices, as shown in Figure 14. The temporal variation of the flow of the three branches does not describe similar behavior. Moreover, it can be certified that the volumetric flow variations are much more perceptible than the pressure losses, i.e., when comparing the temporal variations of the loss coefficient (Figure 10) with the flow variability, as shown in Figure 14.

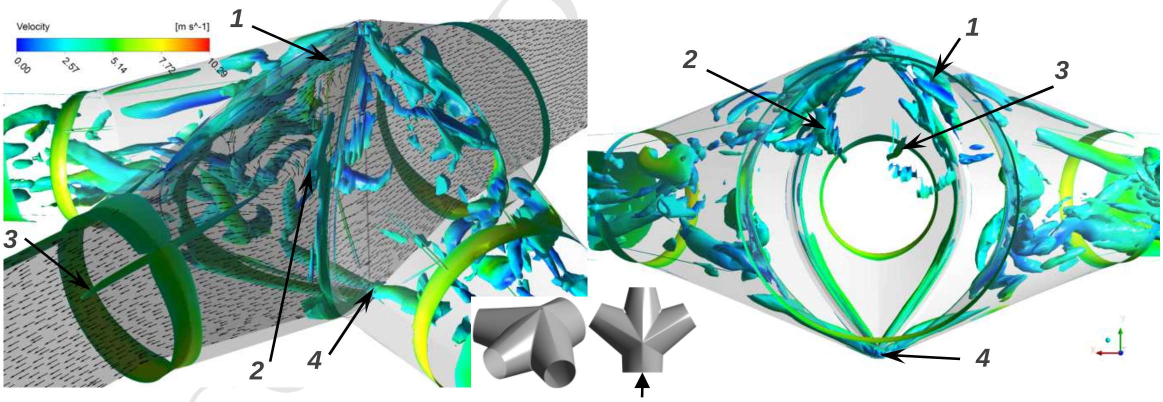

Figure 13 - Turbulence structures for the time 20,90 s; Iso-surface Q = 50 s-² and velocity contour (see the color maps)

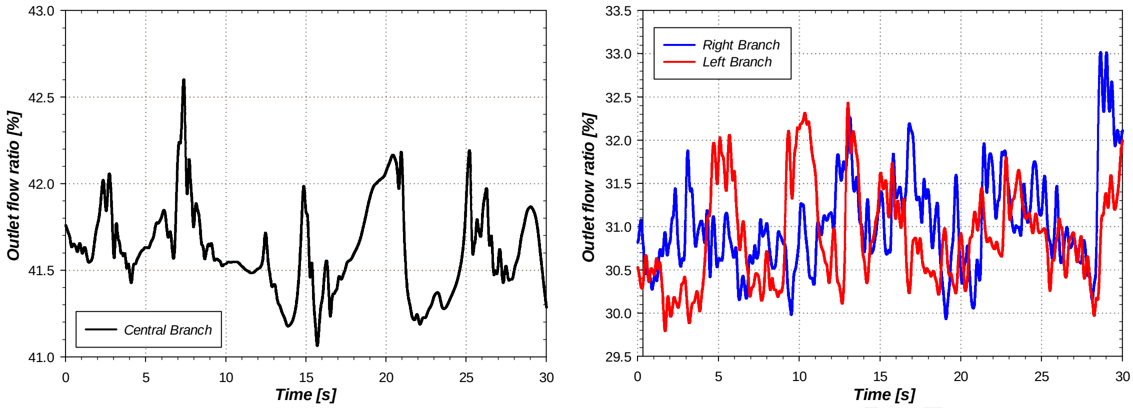

Figure 14 – Flow percentage at the outlet by each ramification for 90 m³/s and interval of time of 0.0 until 30s

Information related to the loss coefficients in trifurcations in transient flow is very limited. In the specialized literature two studies can be found that reported experimental and numerical results on pressure loss behavior: seen in [9] and [10]. Figure 15 shows the result obtained by Ruprecht considering a spherical trifurcation.

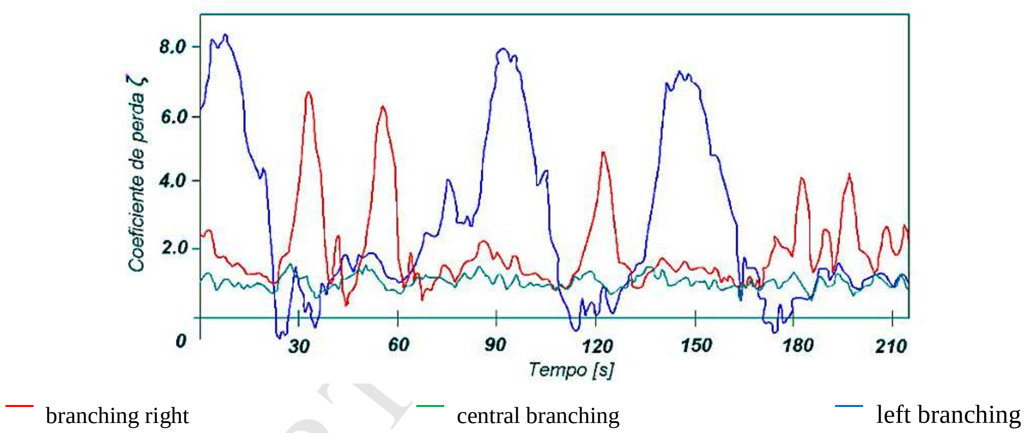

Figure 15 - Experimental pressure drop coefficients of Marshyangdi trifurcation of a non-permanent basis. Source: Ruprecht [10]

The results obtained for the Marsyangdi spherical trifurcation presented higher loss coefficients in the right and left branches. The results for the loss coefficient in the Marsyangdi trifurcation are higher compared with the numerical results in this work for all ramifications due to the geometry of the Marsyangdi being composed of a spherical core without a conical geometrical transition.

Finally, Figure 16a shows the flow variation in the numerical results of Ruprecht’s et al [7] research. In this graph one can observe a better flow distribution (%), in a time of around 80 seconds. In Figure 16b the results of the Gurara trifurcation are displayed, where a higher difference between the central and the laterals flows is observed. In the trifurcation analyzed by Ruprecht, it is possible to see great variations between the right and left ramifications. The numerical approach in Gurara presented minor differences resulting in more stable conditions, as can be seen in Figure 16.

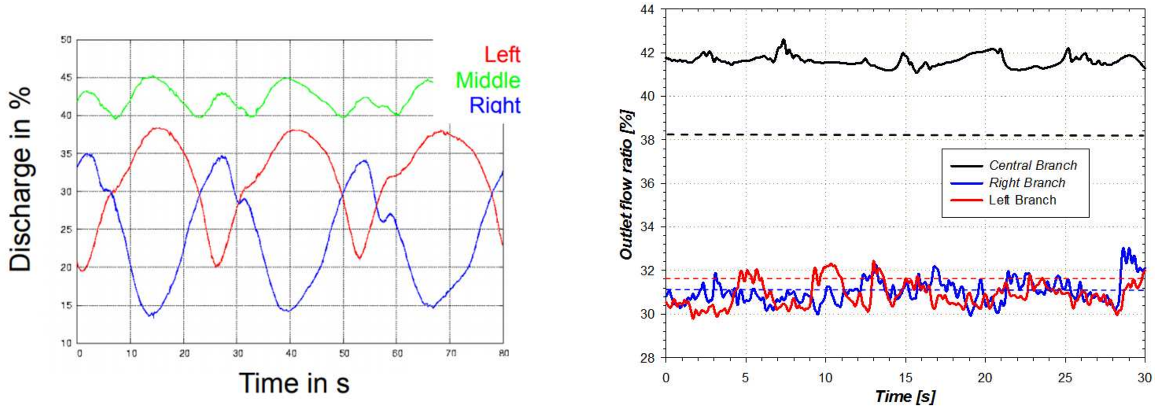

(a) (b)

Figure 16- a) Volumetric flow, Ruprecht [10] b) Volumetric flow % Trifurcation Gurara (the dash line representing of solution in steady state)

4. Conclusions

The trifurcation employment has particular characteristics for each project, resulting in different geometries, even when all of them perform the same function. When the values of the diameter ratio, pressure or flow are different, the loss coefficients and the flow variations can have major differences in the results. Therefore, a strict validation of the numerical results of the trifurcation of Gurara - ALSTOM® can only be performed with a reduced model of experimental data. However, the approach based on CFD, carefully carried out, based on good mesh analysis, can be an appropriate choice of turbulence models, boundary conditions and other parameters, where the numerical and theoretical analyses should be strongly based on the literature and on own experience of the research group.

The results from the numerical analysis of the Gurara-Nigeria project is calculated at the operating point and beyond in order to have a wide range of results for one later comparison with other numerical and experimental results of pressure losses. However, many results (experimental and numerical) are only calculated at the design point.

On the other hand, in order to generalize the results for the particular conditions of each trifurcation, the loss coefficient correlates with the Reynolds number for the steady state, and for the non-stationary state, comparisons were made according to the variation in the total loss coefficient at the time, by the flow.

There is very little information related to the loss coefficients in trifurcations in transient flow. In specialized literature two studies are found that report the experimental and numerical results about the behavior of pressure loss: Ruprechs et al [10] and Tate et al [9]. For the results obtained by Ruprechs considering one spherical trifurcation, the experimental data were obtained based on a smaller scale model with an acquisition time of 210 s, as seen in Figure 15.

5. Acknowledgment

Special Thanks for the contribution of colleagues Outi Supponen, PhD Student in EPFL and Roberto Meira Jr., PhD Student in UNIFEI.

References

[1] AHMED, S. Head Loss in Symmetrical Bifurcations. [s.l.] University of British Columbia, 1965.

[2] MAYR, D. Hydraulische Untersushungen An Dreifachrohrverzweigungen (Trifurcatoren). [s.l.] Technischen Universität Graz, 2002.

[3] GLADWELL, J. S.; TINNEY, R. E. Hydraulic Studies of Large Penstock Trifurcation. Journal of the Power Division, v. 91, n. 1, p. 59–80, 1965.

[4] BERNER, W. Trifurkation, Druckverluste im Verteil- und Sammelbetrieb, Bericht Nr. WT-70-401. [s.l: s.n.].

[5] RAO A.R.; KUMAR B. Energy losses at pipe trifurcations. Technical Note. Urban Water Journal, Vol. 6, No.4, p 333-340. 2009.

[6] WOOD D.J, REDDY L.S., FUNK J.E. Modeling pipe networks dominated by junctions. J Hydraulic Eng; 119(8):949–958. 1993.

[7] LIGGETT J.A. Discussion of "Modeling pipe networks dominated by junctions" by don j. wood, l. srinivasa reddy, and je funk.vol. 119, no. 8. J Hydraul Eng 1994; 120(12):1486–1489. 1993.

[8] RICHTER, A. Energy Head Losses due to a Spherical Pipe Junction for a Power Plant. IAHR Symposium 1988. Anais. Trondheim: 1988.

[9] TATE, C. H. J.; MCGEE, R. G. Fort Peck Tunnel No. 1 Rehabilitation Fort Peck Dam, Montana. Fort Peck: [s.n.].

[10] RUPRECHT, A.; HELMRICH, T.; BUNTIC, I. Very Large Eddy Simulation for the Prediction of Unsteady Vortex Motion. Conference on Modelling Fluid Flow. Anais. Budapest: 2003

[11] JOEPPEN, A. Numerische Berechnung der Strömung in Dreifachrohrverzweigungen (Trifurkatoren). Vienna: [s.n.].

[12] CASARTELLI, E.; LEDERGERBER, N. Aspects of the numerical simulation for the flow in penstocks. IGHEM 2010. Anais.Roorkee: 2010.

[13] DOBLER, W. Hydraulic Investigations of a Y-Bifurcator. [s.l.] Graz University of Technology, 2012.

[14] LASMINTO, U. Comparative Similarity Study on Local Losses of Hydraulic Model with Different Scale Factors. [s.l.] Graz University of Technology, 2012.

[15] WANG, H. Head Losses Resulting From Flow Through WYES and Maniflods. [s.l.] University of British Columbia, 1967.

[16] COX-STOUFFER, S. K. Numerical Simulation of Injection and Mixing in Supersonic Flow. [s.l.] Virginia Polytechnic Institute and State University, 1997.

[17] FONSECA, C. et al. Numerical Approximations for the Structured Thixotropic Fluids in an Abrupt Planar Expansion. International Congress of Mechanical Engineering (COBEM 2013). Anais...Ribeirão Preto: 2013.

[18] VINCHURKAR, S.; LONGEST, P. W. Evaluation of Hexahedral, Prismatic and Hybrid mesh Styles for Simulating Respiratory Aerosol Dynamics. Computers & Fluids, v. 37, p. 317–331, 2008.

[19] ROUCHE, P.J.;Perspective: A Method for Uniform Reporting of Grid Refinement Studies. Journal of Fluids Engineering, Volume 116(3), p. 405-413. 1994.

[20] https://www.grc.nasa.gov/www/wind/valid/tutorial/spatconv.html. 2018

[21] KLASINC, R.; HEIGERTH, G.; MAYR, D. Musi trifurcation, Hydraulic model test. [s.l: s.n.].

[22] MENTER, F. R.; EGOROV, Y. The Scale-Adaptive Simulation Method for Unsteady Turbulent Flow Predictions. Part 1: Theory and Model Description. Flow Turbulence Combust, v. 85, p. 113–138, 2010.

[23] HOLMÉN, V. Methods for Vortex Identification. 2012.

[24] KOLÁR, V. Vortex Identification: New Requirements and Limitations. International Journal of Heat and Fluid Flow, v. 28, n. 4, p. 638–652, 2007.

Numerical Analysis for Detecting Head Losses in Trifurcations of High Head in Hydropower Plants

Carlos Andres Aguirre
Federal University of Itajubá
Institute of Mechanical Engineering
Itajubá, Minas Gerais, Brazil

Ramiro G. Ramirez
Federal University of Itajubá
Institute of Mechanical Engineering
Itajubá, Minas Gerais, Brazil

Waldir de Oliveira
Federal University of Itajubá
Institute of Mechanical Engineering
Itajubá, Minas Gerais, Brazil

François Avellan
Ecole Polytchnique Fédéralede Lausanne, Switzerland

HIGHLIGHTS

- Analysis of mesh non structured and structured mesh.
- Analysis of the pressure coefficient in a transient state, using SAS SST turbulence models.
- Analysis of the vortex flow, obtained from of the transients simulations CFD. This analysis was only reported by RUPRECHT, A.; HELMRICH, T.; BUNTIC, I. Very Large Eddy Simulation for the Prediction of Unsteady Vortex Motion. Conference on Modeling Fluid Flow. Proceedings, Budapest: 2003.
- Validation of the results obtained with other numerical and experimental data results previous researches, beside a thorough review of the literature